



# Investigation into tensile hysteresis of polyurethane-containing textile substrates for coated strain sensors

Qiao Li<sup>a</sup>, Yuchi Wang<sup>a</sup>, Shen Jiang<sup>a</sup>, Ting Li<sup>a</sup>, Xin Ding<sup>a</sup>, Xiaoming Tao<sup>b,\*</sup>, Xi Wang<sup>c,\*</sup>

<sup>a</sup> Key Laboratory of Textile Science & Technology, Ministry of Education, College of Textiles, Donghua University, Shanghai 201620, China

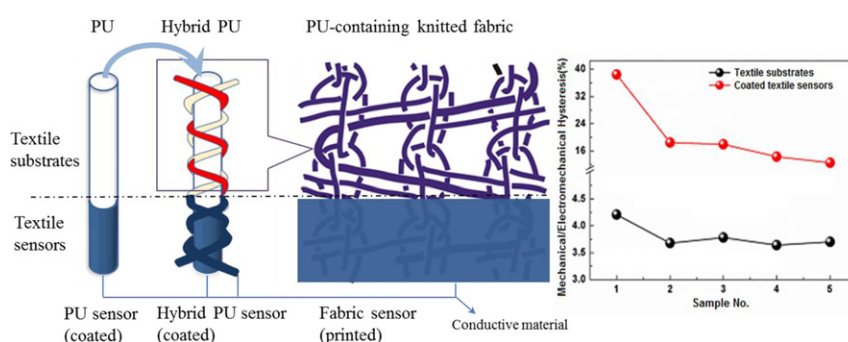
<sup>b</sup> Institute of Textiles and Clothing, The Hong Kong Polytechnic University, Hong Kong

<sup>c</sup> Engineering Research Center of Digitized Textile & Apparel Technology, Ministry of Education, College of Information Science and Technology, Donghua University, Shanghai 201620, China

## HIGHLIGHTS

- A progressive investigation into hysteresis of polyurethane-containing textiles and their coated sensors were presented.
- Fibers, yarn structure and fabric construction together affect the mechanical hysteresis of the textile substrates.
- Reducing mechanical hysteresis of the textiles is effective to lower electromechanical hysteresis of their coated sensors.

## GRAPHICAL ABSTRACT



## ARTICLE INFO

### Article history:

Received 31 October 2019

Received in revised form 20 December 2019

Accepted 21 December 2019

Available online 24 December 2019

### Keywords:

Polyurethane-containing textile

Textile substrates

Mechanical hysteresis

Coated sensors

Electromechanical hysteresis

## ABSTRACT

Flexible sensors based on the highly elastic Polyurethane (PU)-containing textile substrates have been frequently incorporated in enormous wearable applications. However, the desirable sensing properties such as stable sensitivity, small hysteresis and good repeatability depend on the mechanical resilience of the textile substrates. This paper conducts a systematic investigation into the mechanical hysteresis of the PU-containing textile substrates, from fibers to yarns and then fabrics. The impact of fiber materials, yarn structures, and fabric constructions on the overall tensile properties of the PU-containing substrates were examined. It was found that fibers of high elasticity, stable yarn structure with excellent recovery, as well as appropriate fabric construction are effective to reduce the mechanical hysteresis of the textile substrates. Coated strain sensors based on different substrates were then fabricated. Results show that smaller mechanical hysteresis of the PU-containing substrates generally led to lower electromechanical hysteresis and better repeatability of sensors. This paper gives all-round consideration of the fibers and structure features of substrates to provide recommendation for reducing mechanical and electromechanical hysteresis of sensors based on PU-containing textiles and benefiting the design and optimization of other flexible sensors.

© 2019 The Authors. Published by Elsevier Ltd. This is an open access article under the CC BY license (<http://creativecommons.org/licenses/by/4.0/>).

## 1. Introduction

Textiles are favorable supporting substrates for wearable applications. Due to the merits of light weight, excellent permeability, washability, flexibility, as well as comfortability and deformability to

\* Corresponding authors.

E-mail addresses: [xiao-ming.tao@polyu.edu.hk](mailto:xiao-ming.tao@polyu.edu.hk) (X. Tao), [xiwang@dhu.edu.cn](mailto:xiwang@dhu.edu.cn) (X. Wang).

conform the curved human bodies [1–3], textile substrates have been successfully integrated in enormous flexible electronics. Fabric electrodes [4–6], circuits [7–10], transistors [11], antennas [12,13], sensors and actuators [14–19], energy harvesting units [20,21], as well as conversion and storage systems [22–25], have together initiated vast applications such as continuous and long-term health monitoring system [26–28], human-machine interaction [29–31] and multi-functional artificially electronic skin [4,32–34], etc..

As substrates of flexible electronics, textiles are required to return to initial state in idle, which is generally realized by adopting looped knitted structure, as well as incorporation of elastomeric fabrics/yarns/fibers. For instance, the polyurethane (PU) yarns have been broadly used in the textile industry to manufacture various elastic yarns and fabrics [35]. Commercial PU yarns are capable of being elongated over 100% strain and sustain a superior fatigue life of over 1,000,000 cycles at 20% strain. Due to high stretchability, flexibility, durability, biocompatibility, and lightweight, PU yarns have been boosting the designs and applications of a variety of wearable or flexible sensors. For instances, PU yarns have been incorporated in substrates to achieve elastic fabric circuit (boards) and stretchy sensors [4,36–38], either for health care [39,40] or provide feedback to facilitate sports training [41–43]. As carrier of the functional materials, textile substrates not only affect mechanical resilience of the textile electronics, but also have a strong impact on the stability of the electromechanical sensing behaviors [44]. Besides the interaction between the textile substrates and the functional materials [24], published works reveal that fabric-based wearable sensors have been suffering from hysteretic response owing to viscoelastic nature of the textile materials, which impairs the accuracy of the sensors especially during dynamic loading. In particular, the fabric strain sensors based on PU-containing knitted fabrics have been extensively studied [14–17,45,46] for the approximately linear response to strain, large strain range that can fully cover all human skin elongation of 3% to 54%, satisfactory gauge factor [47], as well as excellent durability especially under a large deformation [48]. However, the sensors consistently suffer from larger hysteresis and poor repeatability due to the viscoelastic nature of the fabric/fiber substrates and the conductive material [49]. Hence, in terms of optimizing the sensing performance, it's demanding to analyze the viscoelasticity of textile substrates, as well as specify the factors related to mechanical and electromechanical hysteresis of textile sensors.

Since the electromechanical behavior of the coated sensor has been reported as influenced by mechanical property of the textile substrates [50,51], mechanical hysteresis of the textile substrates will be primarily studied, for which several aspects are to be considered. First, inherent raw fiber materials, i.e., the PU yarns are hysteretic due to the characteristic interchange of micro-phases between hard and soft segments while being cyclically stretched. Secondly, mechanical properties of yarn materials significantly altered before and after disappearances of yarns crimps during elongation [52]. Third, when yarns are straightened, more contact points and higher compression among fibers lead to higher friction [53,54], which takes more time of the whole structure to recovery [55,56]. Hence, it can be qualitatively suggested that the mechanical hysteresis of textile substrates depends on both the amount of elastic material incorporated and the structural design of the textiles [57,58].

To specify the factors related to the mechanical hysteresis of the textile substrates, this paper will conduct a systematic investigation into the mechanical hysteresis of the PU-containing textile substrates and provide recommendations for lowering the electromechanical hysteresis of coated strain sensors. The following work specify in series the effects of fiber materials, yarn structures, and fabric constructions on the overall tensile behavior of the elastic textiles, including bare and hybrid PU yarns and PU-containing knitted fabrics [53]. Recommendations on lowering the mechanical hysteresis of the fabric substrates will be made according to the experimental results and analysis. Then, coated strain sensors based on the textile substrates, i.e., bare PU yarns, hybrid PU yarns and PU-containing fabrics, will be prepared by coating

conductive nanomaterials on the substrates and characterized. The observed effects of fiber material and structure of the substrates on mechanical hysteresis will be further considered to reduce the electromechanical hysteresis of the sensors. This study will help researchers to understand the effects of structures, materials and the interaction within on the mechanical and electromechanical properties of coated textile strain sensors based on PU-containing textiles, and provide a practical reference on the design and optimization of other elastic fabrics and sensor products.

## 2. Materials and experiments

### 2.1. Selection of PU-containing textiles

Commercial PU yarns with different linear densities ranging from 40D to 840D were bought from Invista Co., Ltd., Guangzhou, China. One layer of polyamide (PA) multifilaments were wrapped around PU yarns in one direction with a direct twisting device (provided by Zhende Medical Co., Ltd., Shaoxing, China), forming the single-covered hybrid yarns, which were further covered by a second layer of PA filaments wrapped in the opposite direction to make the double-covered hybrid yarns. Totally 26 knitted fabric samples consisting of bare or hybrid PU yarns were randomly purchased from the market.

### 2.2. Fabrication of PU-containing textile strain sensors

Strain sensors based on PU-containing textile substrates were fabricated through 2 ways of coating. PPy conductive materials were coated on the yarn-type substrates, i.e., PU and hybrid PU yarns, through chemical treatments. The yarns were firstly alkali-treated with NaOH solution, then immersed in a mixed solution of pyrrole, anthraquinone-2-sulfonic acid sodium salt (AQSA), and FeCl<sub>3</sub>, where in-situ polymerization was carried out, and finally dried in an oven. For fabric substrates, composite of carbon nano-particle (CNP)/silicone elastomer (SE)/silicone oil (SO) was uniformly printed on target side with a screen printing machine (Guangdong Ever Bright Printing Machine Fty Ltd., Guangzhou, China), whose mesh size of screen was 1000 holes per square inch. The coated fabric sensors were then cured at 100 °C for 1 h.

### 2.3. Characterization

Tensile test of the selected elastic PU-containing textile substrates (PU, hybrid PU and PU-containing fabric) was conducted under room temperature of 20 °C and a relative humidity of 65%. The samples were clamped and cyclically stretched by a YG026MB electronic fabric strength tester (Wenzhou Fang Yuan Instrument Co. Ltd., Wenzhou, Zhejiang, China). The gauge length and tensile velocity for yarns was set to 50 mm and 200 mm/min, respectively. The mechanical hysteresis of the samples  $H$  was obtained from the last cycle of the tension-strain curve and determined using the equation of  $H =$

$$\frac{|F_{\varepsilon_{0up}} - F_{\varepsilon_{0down}}|_{\max}}{F_{\max} - F_{\min}} \times 100(\%),$$

where  $|F_{\varepsilon_{0up}} - F_{\varepsilon_{0down}}|_{\max}$  is the largest difference of the tension for same strain between the uploading and down-loading conditions,  $F_{\max}$  and  $F_{\min}$  are the upper and lower limits of measured tension, respectively.

Sensing behavior of the yarn- and fabric-based strain sensors was investigated with the exactly same experimental setup aforementioned. Since the sensing area of the fabric sensors in this work was 20 mm \* 20 mm, the gauge length and corresponding testing speed for PU-containing fabrics was chosen as 20 mm and 90 mm/min, respectively. The resistance of the coated strain sensors was acquired and recorded continuously by Agilent 34970A (Agilent Technologies Inc., USA). The electrical hysteresis of the coated strain sensors  $H_s$  was determined as  $H_s = \frac{|R_{\varepsilon_{0up}} - R_{\varepsilon_{0down}}|_{\max}}{R_{\max} - R_{\min}} \times 100(\%),$  where  $|R_{\varepsilon_{0up}} - R_{\varepsilon_{0down}}|_{\max}$

is the maximum difference of the resistance at same strain between the uploading and downloading phases,  $R_{max}$  and  $R_{min}$  represent the highest and lowest electrical resistances, respectively.

Meanwhile, the repeatability of sensors, which describes the ability of a sensor to repeat the observations for same load of strain, was also evaluated by  $\delta_R = \frac{\sigma_{R_{max}}}{R_{max} - R_{min}} \times 100(\%)$ , where  $\sigma_{R_{max}}$  is the variation of electrical resistance at the maximum strain among the first 10 loading-unloading cycles. According to the equation, the less  $\delta_R$  is, the better repeatability the sensor has.  $\delta_R$  was used as representation of repeatability of coated textile sensors since it characterizes the variation of resistance at the maximum strain, which is related to the shift errors of observations at the maximum strain.

The morphology and structural variations of the samples during deformation were tracked through SEM observations made by the TM-3000 scanning electron microscope (Hitachi, Tokyo, Japan), prior to which the specimens were prepared by firstly freeze-fracturing in liquid nitrogen, then a gold coating.

### 3. Results and discussion

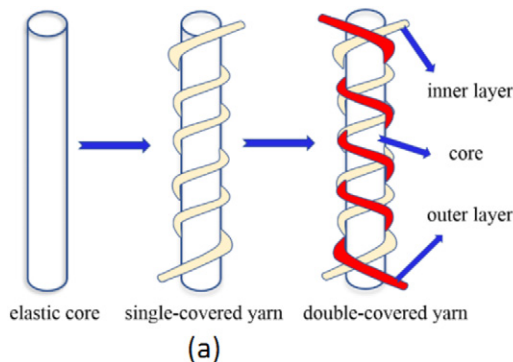
#### 3.1. Hysteresis of bare and hybrid PU yarns

Commercial PU yarns used in this work are of different linear densities ranging from 40D to 840D, low in Young's modulus and support large elongation of as high as 500% strain. Schematic diagram of wrapping PA on PU yarns is demonstrated in Fig. 1a. Compared to the single-covered hybrid yarns, the number of coils per unit length of the double-covered yarns was doubled, which significantly reduced the exposed portion of the core PU yarns. More importantly, the double-covered hybrid PU yarns were more convenient for applications without pre-stabilization, since the tensions induced by wrapping were balanced in length direction according to the setup. Fig. 1b gives an overview of the selected bare PU and hybrid PU yarns with different linear densities. Cyclic tensile tests of the PU and hybrid PU yarns were conducted. The specimens were firstly pretreated by 5 loading-unloading cycles within the strain range of 0–80% to stabilize the mechanical property and then calibrated by 10 cycles of stretch within 0–60% strain. The maximum strain of 60% for calibration is chosen according to the reported extension range of human skin as from 3% to 55% [59]. The tension and axial strain were recorded simultaneously during the test. The tension-strain curves of both bare PU and hybrid PU yarns for the last calibration cycle were plotted in Fig. 2. The reason for selecting the last loop is that, internal frictions of the macromolecular chains among fibers and yarns tended to be smaller and more stable after repeated orientation rearrangement (stretching), which could lead to stable tension-strain curve and smaller mechanical hysteresis.

It can be observed from Fig. 2a that, the tension of all the bare PU yarns increased almost linearly with strain. Since tensile stress of the

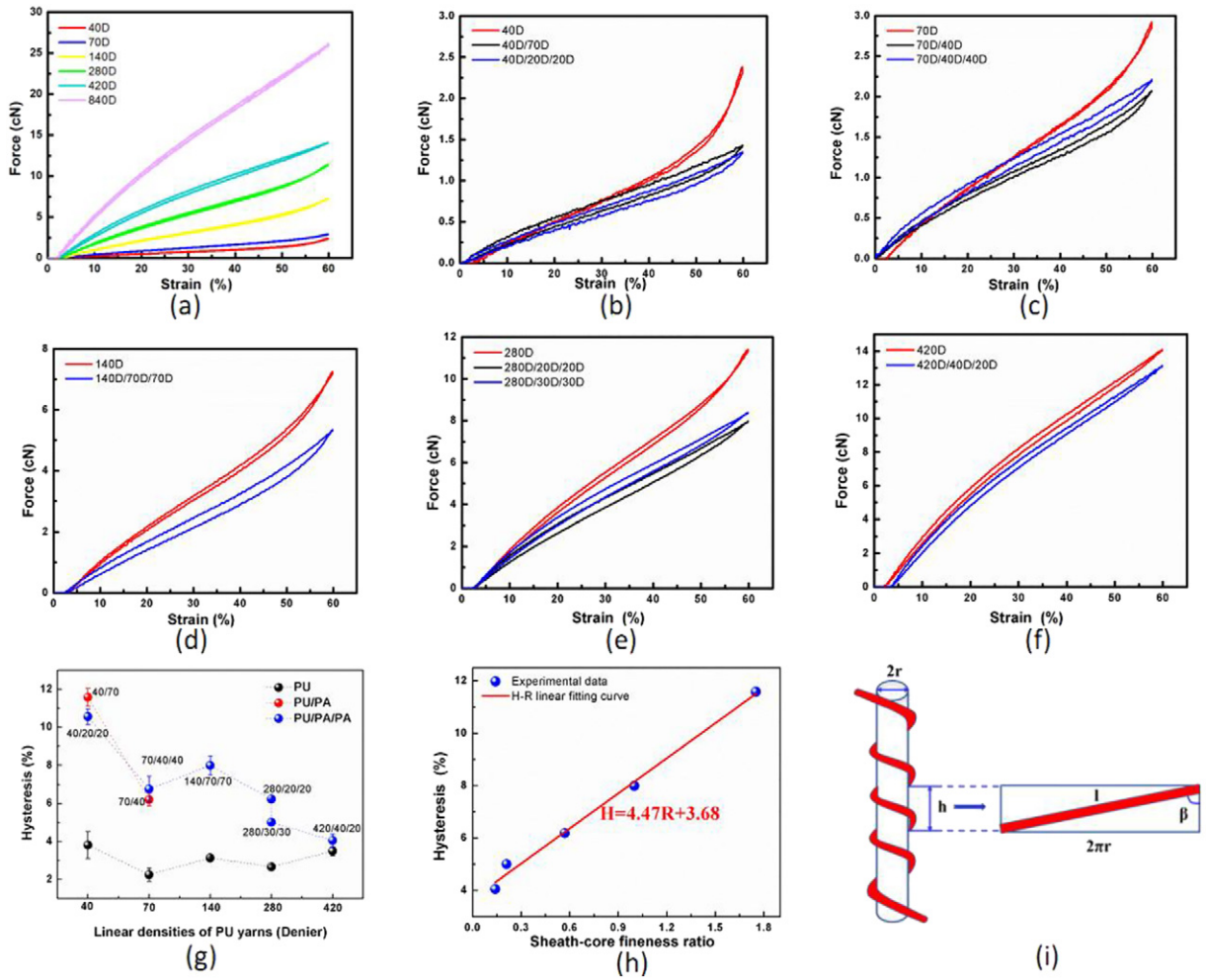
purchased PU can be considered as a constant value of 0.05cN/tex, the difference in tension at same strain can be attributed to variant fineness. Mechanical hysteresis of yarns was observed from the Fig. 2a) and plotted in Fig. 2g. It can be found that mechanical hysteresis of the bare PU yarns with diverse linear densities were close to each other, ranging from  $2.52 \pm 0.35\%$  to  $3.81 \pm 0.71\%$ , indicating the tensile hysteresis is dominated by the nature of material itself, other than their fineness.

Fig. 2b-f further displays the similar approximately linear tension-strain curves of the hybrid PU yarns. However, stiffness of hybrid PU yarns can be found as a little smaller than that of bare PU samples, which is believed caused by the crimped structure of PU core in hybrid PU yarns. Two more findings were observed. First, linear relationship was observed between the mechanical hysteresis and sheath-core fineness ratio (defined by  $R = (D_{layer1} + D_{layer2})/D_{core}$ , where  $D_{layer}$  and  $D_{core}$  are deniers of the sheath and core, respectively), which can be well-fitted by the linear form of  $H = 4.47R + 3.68$ , and the  $r^2$  was observed as high as 0.991. This result suggests lowering the sheath-core fineness ratio would help to reduce the mechanical hysteresis of hybrid PU yarns. Moreover, samples with same fineness ratio and linear densities of 420D/40D/20D were found with lower mechanical hysteresis than that with linear densities of 280D/20D/20D. The reason can be attributed to stable structure established by more rigid coarse PU core, which reduced the possibility of relative slip between the fibers and the yarn. Secondly, better coverage of the wrapped layers tended to lead to smaller hysteresis of the PU yarns. As shown in table S1, the mechanical hysteresis of the samples with larger twist of the PA filaments was found below the mean value (7.29%) of all the hybrid PU yarns and vice versa. To understand this, suppose PA filaments with minor diameters were evenly wound around the PU core in a helical pattern with a constant twist  $T$ . The helical angle  $\beta$  can be determined by  $\tan\beta = 2\pi rT$ , where  $r$  is the radius of the core. When stretched, both the PU core and PA filaments of the hybrid PU yarns were elongated and deformed, which caused relative slipping between them back and forth during loading and unloading phases, respectively. Generally, longer slipping distances means longer time under dynamic friction, which takes longer time for yarns to recover/approach the initial status. It can be figured that slipping distance of PA filaments along core PU yarn is smaller for hybrid PU yarns with a higher coverage, and longer for that with a smaller coverage. To understand this result, consider a constant strain applied on the hybrid PU yarns in Fig. 2i, the total consumed energy  $W$  by assumed constant friction during the slipping of a single coil can be given as  $W = f \cdot \int_0^{2\pi} x \cdot (\frac{1}{\tan\beta'} - \frac{1}{\tan\beta}) dx = \frac{2f\pi r^2 \epsilon}{\tan\beta}$ , where  $f$  is the friction assumed to be constant here,  $\beta'$  is the helical angle when a strain of  $\epsilon$  is applied to the yarns. It can be easily seen that the consumed energy is a decreasing function of helical angle  $\beta$ . This could explain that the double-covered hybrid PU yarns were observed with a lower hysteresis value of  $6.76 \pm 1.05\%$  while that of the single-wrapped ones were determined as  $8.89 \pm 1.35\%$ .



Samples	Linear Density (Denier)
PU	40, 70, 140, 280, 420, 840
PU/PA	40/70, 70/40
PU/PA/PA	40/20/20, 70/40/40, 140/70/70, 280/20/20, 280/30/30, 420/40/20

Fig. 1. Selected PU yarns. (a) Schematic diagram of wrapping PA on PU yarns to form hybrid PU yarns. (b) Linear density of bare PU and hybrid PU yarns.



**Fig. 2.** Tensile properties of the bare and hybrid PU yarns. (a) Tension-strain curves of the bare PU yarns; (b)–(f) Tension-strain curves of the hybrid PU yarns with different linear densities; (g) Mechanical hysteresis of the bare PU and hybrid PU yarns; (h) Hysteresis-finesse relation of the hybrid yarns; (i) Yarn twisting of the hybrid yarns.

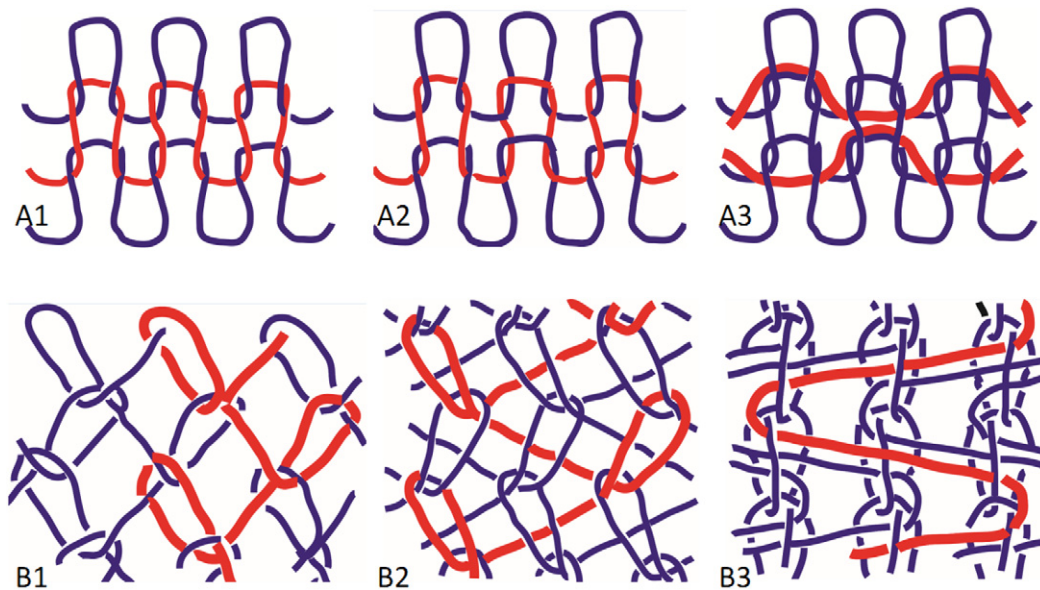


**Fig. 3.** Different knitted structures (A1-Plain; A2-Rib; A3-Fleecy; B1-Tricot; B2-Cord; B3-Inlay) of the selected elastic PU-containing fabrics.

### 3.2. Hysteresis of PU-containing fabrics

Totally 26 pieces of PU-containing knitted fabrics were randomly purchased. The constructions and specifications of the samples are plotted in Fig. 3 and listed in table S2. All the samples were grouped into weft- and warp-knit fabrics, termed as A and B, respectively. Samples of group A were fabricated by knitting or inlaying the elastic PU yarns into the fabric along the weft case, while for samples of B group, the elastic yarns were fed into the constructions in the warp direction [60]. All fabric samples incorporated PU yarns as the core, which were mixed with hybrid yarns covered by of PA, polyester (PET) filaments or cotton (C) yarns. Tensile tests were carried out in both wale and course direction of the PU-containing elastic fabrics except A3 and B3 samples, which were designed with anisotropic elasticity between horizontal and vertical directions. Tension-strain curves of all the specimens along both directions were observed and shown in Fig. 4.

Fig. 4a-d present nonlinear tension-strain curves in similar shape corresponding to fabrics A1, A2, B1, and B2 in both directions regardless of differences in constructions and fabric densities. It can be found that except for 1st cycle, the tension-strain curves of 2nd and later cycles showed acceptable repeatability. As indicated by tension, stiffness of fabrics differed during stretch (caused by different deformation styles), between the wale and course cases, as well as among different samples, which is believed due to the various fiber materials, geometrical structures and fabric densities. Higher hysteresis (as plotted in Fig. 5a) of about  $15.52 \pm 2.87\%$  was observed compared to the PU yarns. In contrast, tension-strain curves of A3 and B3 samples (fleecy and inlay structures) with in-laid PU yarns were found approximately linear, indicating that PU yarns dominated the mechanical property of these two fabrics. Moreover, comparatively smaller mechanical hysteresis values of  $10.43 \pm 4.01\%$  and  $10.79 \pm 1.43\%$  were observed for A3 and B3 samples, respectively.

To reveal the underlying mechanism of A3 and B3 samples' lower mechanical hysteresis, morphological parameters of the fabrics during loading and unloading phases were examined with microscopic images.

For fleecy fabric (Fig. 5b), the changes in width (wale spacing), height (course spacing), length of the limb as well as angle of the fabric under strains of 0%, 40%, 60% and without external load were plotted in Fig. 5d-f. The initial width of loops of the fleecy fabric was as dense as  $461 \pm 72 \mu\text{m}$ , which was believed induced by the pre-tension provided by hybrid PU yarns along transverse direction. The course spacing, wale spacing and the angle increased monotonically, while limb length first increased and then slightly decreased. The overall increment in loop length showed that ground yarn and laying-in PU yarn were lengthened simultaneously and hence reduced the possibility of transfer of yarns and slipping of interlacing point, which decreased the tension-strain hysteresis of the knitted fabrics. For inlay fabrics (Fig. 5c), wale spacing, course spacing, as well as loop pillar angle were compared among different applied strains in the wale wise and plotted in Fig. 5g-i. The stitch loops tend to conform to the direction of tension, causing the increment in course spacing and reduction in pillar angle, while the maintained wale spacing can be attributed to excellent transverse stability of the fabric. Hence, the elastic yarns and inelastic yarns undertook load/deformation and stabilized the fabric structure in transverse direction, respectively. This division of labor can largely prevent the slipping of interlacing point during stretching, and effectively reduce mechanical hysteresis.

### 3.3. Hysteresis from PU yarns to fabrics

A clear trend of increasing hysteresis from bare PU to hybrid PU yarns and then to the whole PU-containing fabrics can be observed from above. To study the 'transmission' of mechanical hysteresis through different levels of textile substrates, the method of multivariate correlation analysis was implemented. Fleecy fabric (A3) was chosen for demonstration, where comparison was made among hysteresis of the whole fabric, ground fabric, inlay hybrid PU yarn, as well as bare PU core. Eight types of fleecy fabrics with different densities were randomly purchased. Most of the looped and inlay yarns of the fabrics employed PU/PA hybrid yarns while the rest use bare PU yarns (Table S3). Cyclic

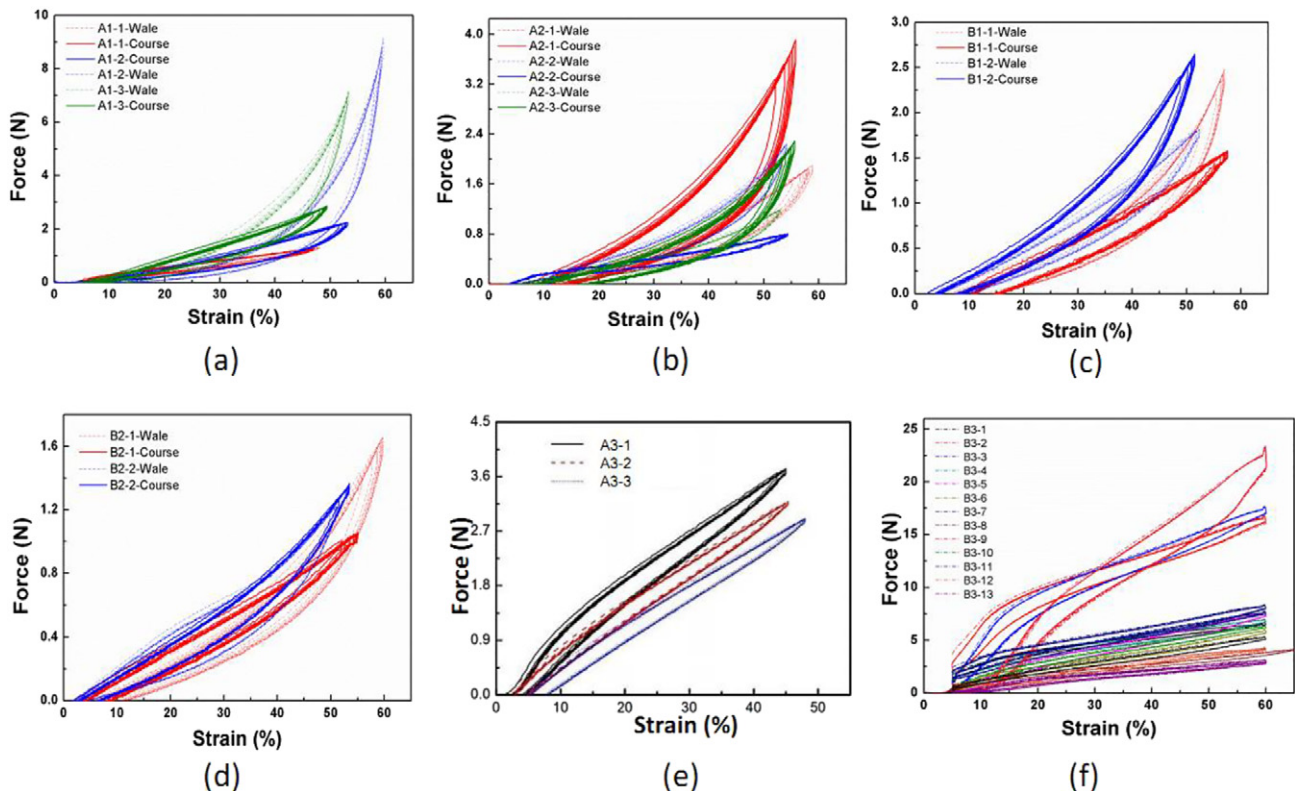


Fig. 4. Tension-strain curves of the PU-containing fabrics with different constructions, i.e., A1-plain (a); A2-rib (b); B1-tricot (c); B2-cord (d), A3-fleecy (e), and B3-inlay (f).

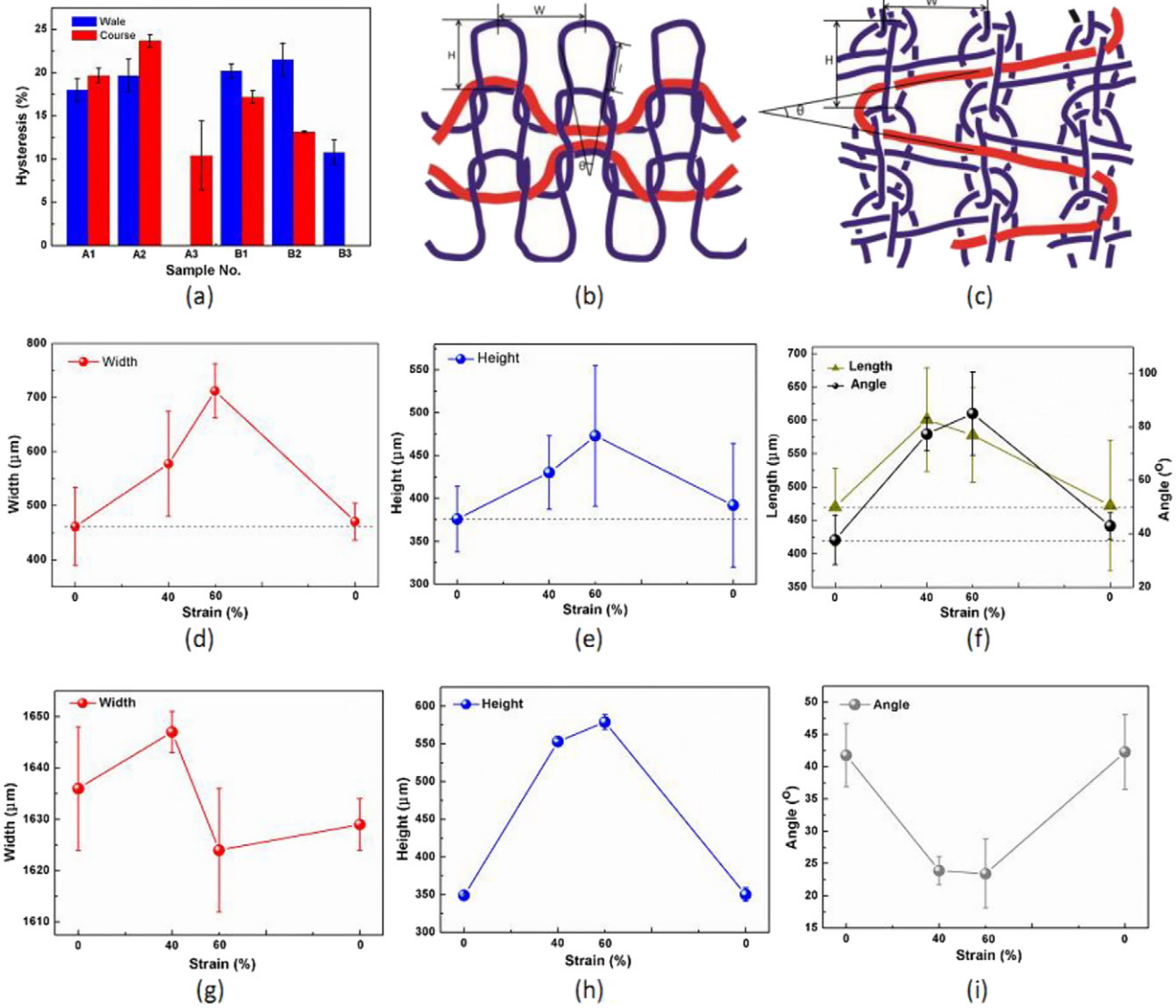


Fig. 5. Hysteresis of the PU-containing fabrics and their influential structural factors. (a) Hysteresis of all the fabrics; (b-c) Geometrical configurations of the fleecy and inlay fabrics. (d-f) Changes in geometrical parameters of the loops in the fleecy fabric. (g-i) Changes in geometrical parameters of the loops in the inlay fabric.

tensile tests were conducted on samples, using the same protocol as aforementioned.

Mechanical hysteresis of the fleecy fabric samples were calculated and plotted in Fig. 6a. It can be easily seen that mechanical hysteresis increased from the bare PU yarns, to hybrid PU yarn, fleecy fabrics, and ground fabric. The averaged mechanical hysteresis were observed as  $2.80 \pm 2.25\%$ ,  $4.16 \pm 1.42\%$ ,  $7.31 \pm 2.25\%$  and  $24.03 \pm 4.75\%$ , for bare

PU yarns, hybrid PU yarns, fleecy fabric and ground jersey fabric (largest), respectively. Pearson correlation coefficients and significances was calculated and summarized in Fig. 6b. Three conclusions can be drawn. First, the mechanical hysteresis of the PU yarns dominated the mechanical hysteresis of the fleecy fabric since there was a strong correlation between them at the 0.05 level. Second, another significant correlation between mechanical hysteresis of the PU core and hybrid PU

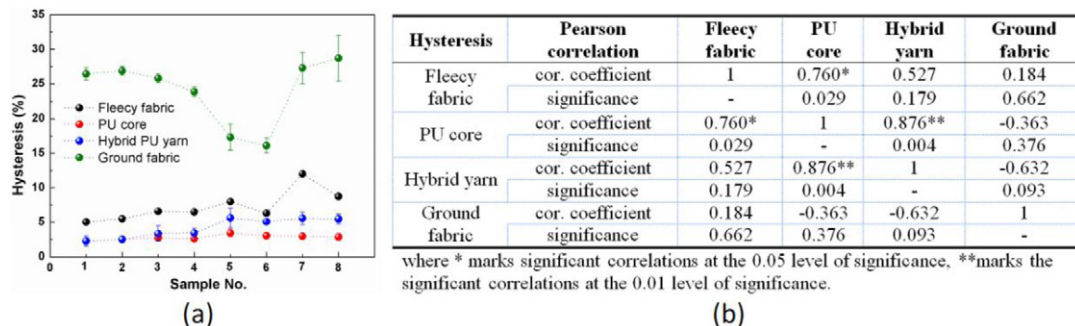


Fig. 6. Mechanical hysteresis (a) and its correlation analysis (b) of the different PU-containing textiles.

yarns can also be found at the level of 0.01. Third, no obvious correlation between the mechanical hysteresis of ground fabric and that of the other three levels of textiles was found, although the involvement of the looped yarns is believed to have increased the mechanical hysteresis of the whole fabric. Fig. 6b further indicates that the PU yarns and inlaid hybrid PU yarns undertook most tension when the whole fabric was stretched, making the tensile properties of the whole fabric close to that of the inlaid yarn. Hence, it can be concluded that lowering the mechanical hysteresis of hybrid PU yarn can effectively reduce the mechanical hysteresis of the whole fabric.

3.4. Electromechanical hysteresis of coated sensors based on textile substrates

Textile strain sensors fabricated by printing or depositing strain-sensitive materials, usually electrically conductive fillers, including metal nanowires [61], conducting polymers [62–65] and carbon (or graphite)-based conductive composites [64–67], on textile substrates (elastic fiber, yarn or fabrics) have been frequently studied. In particular, PU-containing textile substrates have been proven effective to improve the resilience and elasticity of the textile-based sensors. In this work, two commercially available conductive composites were utilized as

sensing materials, i.e., polypyrrole (PPy) and carbon nano-composites. Both materials were low-cost, environmentally friendly and with sufficiently high electrical conductivity to produce desirable variation in resistance under directional load of strain. Bare PU yarns of 840D, hybrid PU yarns (420D/40D/20D) and elastic knitted fabrics with comparatively lower tensile hysteresis were chosen as substrates of textile strain sensors. Fabrications of the coated strain sensors were conducted as aforementioned in the methods section. Fig. 7a–c present SEM images of different textile substrates and corresponding coated strain sensors, respectively. Conductive material can be observed almost evenly distributed on the surface of the PU yarns, PU and PA filaments, as well as the fabric surface.

To determine the mechanical-electrical hysteresis, the coated strain sensors were pretreated and calibrated using same protocols as previously mentioned. The electrical resistance, tension, and axial strain were measured and recorded simultaneously. Fig. 7d–f show the typical curves of tension-strain and resistance-strain of the coated sensors. All the three sensors revealed approximately linear tension-strain relations. However, unlike the linear resistance-strain curve of fabric-based sensors, electrical resistance of the yarn-based sensors increased nonlinearly with applied strain. Gauge factor ( $GF = \frac{\Delta R/R}{\epsilon}$ , where,  $GF$  is gauge factor,  $\Delta R$  is increment of the electrical resistance at the applied

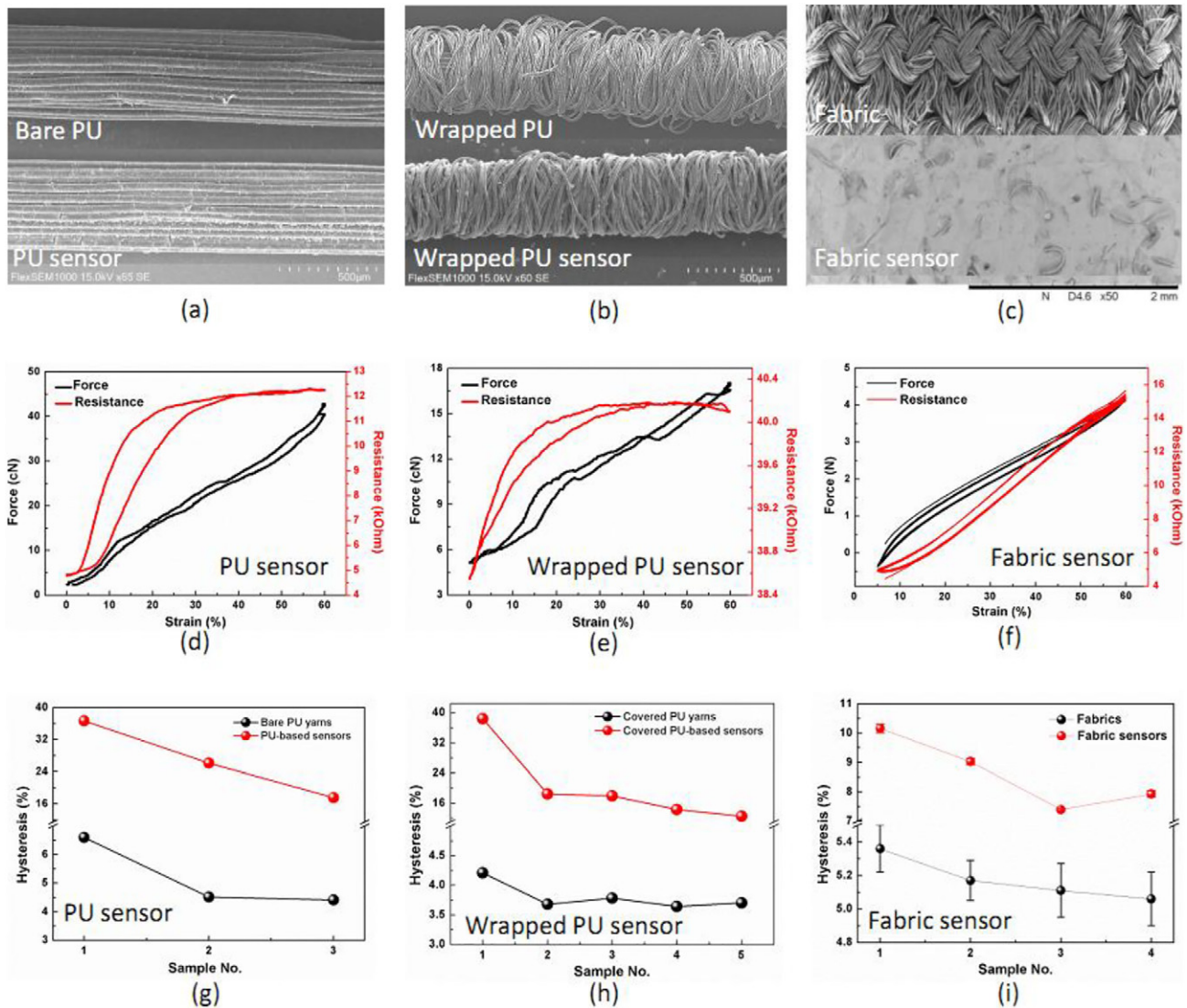


Fig. 7. Coated strain sensors on PU-containing textile substrates. (a–c) SEM images of the bare PU (a), hybrid yarns (b) and fabrics (c) and their resultant sensors. (d–f) Tension and resistance versus strain of the three sensors. (g–i) Hysteresis of each kind of sensors.

strain  $\varepsilon$ ) of PPy coated yarn-based sensors were larger before 30% strain, and rapidly decreased after, compared to the stable value of 3.67 for fabric-based sensors. The possible reasons for this result may be addressed to different sensing mechanisms for yarn-based and fabric-based sensors, which are further induced by the type of materials, micro/nanostructures, and fabrication process.

Tensile hysteresis were obtained from samples for each kind of sensors and plotted in Fig. 7g-i. Two primary conclusions can be made. First, for each type of sensors, lower mechanical hysteresis of the textile substrates generally led to smaller mechanical-electrical hysteresis of their resultant sensors, indicating that the sensing performance of textile-based sensors was highly affected by the mechanical properties of the textile substrates. Second, despite the similar mechanical hysteresis among different textile substrates, comparatively higher hysteresis of the PPy-coated yarn sensors were observed, showing that other factors such as interfacial binding between conductive materials and substrates may be influencing the electromechanical hysteresis. To prove this, we considered the equivalent electrical resistance  $R$  of the conductive composite based on tunneling current [68],  $R = \left(\frac{L}{N}\right) \frac{8\pi h s}{3a^2 \gamma e^2} \exp(\gamma s)$ , where  $R$

is the equivalent resistance of the composite;  $L$  is the number of conductive particles forming a single conductive path parallel to the conductive direction;  $N$  is the number of conductive pathways;  $h$  is the Planck's constant;  $s$  is the least distance between conductive particles or domains;  $a^2$  is the effective cross-sectional area in which the tunneling current passes through;  $e$  is the electron charge, and  $\gamma$  is defined as  $\gamma = \frac{4\pi}{h} \sqrt{2m\phi}$ , in which  $m$  is the electron mass and  $\phi$  is the height of potential barrier between adjacent conductive particles. This equation generally governs the correlation between elongation and resistance for conductive material based on composites with conductive particles inside. Since  $\gamma > 0$ , the equivalent electrical resistance  $R$  is actually a convex function of elongation  $s$  with an increasing gauge factor, while the real observed curves of strain-resistance for the yarn sensors are concave (Fig. 7d and e, gauge factor is decreasing during loading). The observation of resistances' being 'insensitive' to elongation indicates that, there are either detachment of coated sensing materials on disparate time scales or cracks controlled by strain field on the surface of yarns, both effect the interaction between materials and could be caused by ubiquitous frictional sliding among fibers and PU core yarns during stretching. In contrast, the fabric strain sensors in Fig. 7f shows linear response of resistance (slight convex), which may be attributed to a more stable support and solid contact provided by fabrics, which are of higher dimension than yarns. Hence, it can be concluded that hysteresis was mainly caused by not only the viscoelastic nature of textiles but also the interaction between nanomaterial fillers and substrates [55]. Actually, the deformation of microscopic morphology of the coated material on substrates, which is affected by the bonding conditions between the 2 components, determines the sensing mechanism of those textile sensors. When the coated materials are ideally firmly adhered to fabric substrates, resistance variations are then exclusively caused by the geometric deformation of the fibers. In this scenario, the strain-resistance property of the sensors is governed by the tunneling theory as elaborated above. However, when cracks, slippage and buckling occur on the coated materials, the 'switch effect' takes over the resistance change. The resistance of the whole sensing network increases and decreases as the in-location 'switches' disconnects and reconnects caused by loading and unloading phases of elongation. For sensors in this work, there is a mixture of the above 2 sensing mechanisms, details of which would be explored in detail by another related paper of us.

Furthermore, the repeatability of the coated sensors ( $\delta_R$ ), was observed as 25.01%, 20.68% and 19.56% respectively for No. 1-3 PU sensors, which were generally correlated with the electromechanical hysteresis of the corresponding PU sensors (36.68%, 26.17% and 17.60%, as demonstrated in Fig. 7g). Similar correlation can be obtained with the observed

repeatability of 24.36%, 20.61%, 21.45%, 19.26% and 19.81% for wrapped PU sensors No. 1-5. The finding is theoretically reasonable, since both repeatability and mechanical/electromechanical hysteresis are caused by the viscoelasticity of component materials, only that the former reflects chronic variation in resistance among multiple cycles while the latter reveals the discrepancy during one single cycle. However, for fabric sensors whose electromechanical hysteresis are mainly lower than 10%, no such correlation between repeatability and hysteresis was found (repeatability were observed as 9.69%, 11.34%, 8.07%, 7.65% for fabric sensors No. 1-4). It's believed that the more complex structure and different sensing mechanism of the fabric sensors led to this result.

#### 4. Conclusion

This paper delivers a systematic investigation with both experimental and theoretical analysis on the mechanical hysteresis of the PU-containing textile substrates as well as electromechanical hysteresis of the corresponding coated sensors.

Through tracking along tensile properties of bare PU yarns, hybrid PU yarns, to PU-containing fleecy fabrics and ground fabrics, several findings were observed. First, bare PU yarns with a large difference in linear densities ranging from 40D to 840D were found with similar and small mechanical hysteresis, showing that the tensile hysteresis is determined by the nature of PU material itself and has little/weak correlation with their fineness. Further, lowering the sheath-core fineness ratio will be effective to reduce the mechanical hysteresis of hybrid PU yarns. Moreover, sufficient coverage of the PU core with wrapped layers could also effectively prevent the energy consumed during relative sliding between core and wrapping layers, hence will also reduce the mechanical hysteresis of the hybrid PU yarns. Elastic fabrics of fleecy and inlay structures demonstrated a favorable linear tension-strain curves and comparatively smaller mechanical hysteresis since intrinsic PU yarns bore the tension. According to multivariate correlation analysis, hysteresis of the PU core was found dominating the hysteresis of the fleecy fabric, while lowering the tension-strain hysteresis of hybrid yarn would be effective to reduce the hysteresis of the whole fabric.

Yarn-based and fabric-based coated strain sensors were fabricated. Since lower mechanical hysteresis of the textile substrates generally led to smaller electromechanical hysteresis of their resultant sensors, it's recommended to lower the mechanical hysteresis of PU-containing substrates according to the above findings. Aside from viscoelastic nature of textiles, complex interaction between coated sensing materials and substrates was also specified as important reason for electromechanical hysteresis of the sensors.

The findings of this work can provide a practical reference on the incorporation of PU-containing textile substrates in textile-based electronics for wearable applications. It can be summarized from the above analysis of influencing factors of the tensile hysteresis of knitted fabrics that, fiber material with high elasticity, the yarn structure with stable mechanical properties and excellent recovery, and appropriate fabric structural parameters are crucial to reduce the mechanical hysteresis of the substrates. Moreover, methodology and results of this study will also help the understanding of structure features, mechanical properties, and their interaction involved in textile substrates and the textile-based sensors.

#### Data availability

The raw/processed data required to reproduce these findings cannot be shared at this time as the data also forms part of another ongoing study.

#### CRedit authorship contribution statement

**Qiao Li:** Conceptualization, Methodology, Investigation, Formal analysis, Writing - original draft, Writing - review & editing,

Supervision. **Yuchi Wang:** Investigation. **Shen Jiang:** Investigation. **Ting Li:** Investigation. **Xin Ding:** Supervision. **Xiaoming Tao:** Conceptualization. **Xi Wang:** Conceptualization, Formal analysis, Writing - original draft, Writing - review & editing.

### Declaration of competing interest

All authors of this work have no commercial or associative interest to declare that represents a conflict of interest in connection with this manuscript submitted.

### Acknowledgment

This research was funded by the National Natural Science Foundation of China (Grant No. 51603039), sponsored by Shanghai Pujiang Program, and supported by the Fundamental Research Funds for the Central Universities, the Key Laboratory of Textile Science and Technology (Donghua University), Ministry of Education, as well as the Initial Research Funds for Young Teachers of Donghua University.

### Appendix A. Supplementary data

Supplementary data to this article can be found online at <https://doi.org/10.1016/j.matdes.2019.108451>.

### References

- [1] Y. Gao, L. Yu, J.C. Yeo, C.T. Lim, Flexible hybrid sensors for health monitoring: materials and mechanisms to render wearability, *Adv. Mater.* (2019) e1902133, <https://doi.org/10.1002/adma.201902133>.
- [2] W. Zeng, L. Shu, Q. Li, S. Chen, F. Wang, X.M. Tao, Fiber-based wearable electronics: a review of materials, fabrication, devices, and applications, *Adv. Mater.* 26 (2014) 5310–5336, <https://doi.org/10.1002/adma.201400633>.
- [3] S. Seyedin, P. Zhang, M. Naebe, S. Qin, J. Chen, X.A. Wang, J.M. Razal, Textile strain sensors: a review of the fabrication technologies, performance evaluation and applications, *Materials Horizons* 6 (2019) 219–249.
- [4] C.L. Choong, M.B. Shim, B.S. Lee, S. Jeon, D.S. Ko, T.H. Kang, J. Bae, S.H. Lee, K.E. Byun, J. Im, Y.J. Jeong, C.E. Park, J.J. Park, U.I. Chung, Highly stretchable resistive pressure sensors using a conductive elastomeric composite on a micropyramid array, *Adv. Mater.* 26 (2014) 3451–3458, <https://doi.org/10.1002/adma.201305182>.
- [5] K. Yang, C. Freeman, R. Torah, S. Beeby, J. Tudor, Screen printed fabric electrode array for wearable functional electrical stimulation, *Sensors Actuators A Phys.* 213 (2014) 108–115, <https://doi.org/10.1016/j.sna.2014.03.025>.
- [6] L. Zhang, M. Fairbanks, T.L. Andrew, Rugged textile electrodes for wearable devices obtained by vapor coating off-the-shelf, plain-woven fabrics, *Adv. Funct. Mater.* 27 (2017).
- [7] K. Cherenack, C. Zysset, T. Kinkeldei, N. Munzenrieder, G. Troster, Woven electronic fibers with sensing and display functions for smart textiles, *Adv. Mater.* (2010) 22 5178–+, <https://doi.org/10.1002/adma.201002159>.
- [8] Q. Li, X.M. Tao, Three-dimensionally deformable, highly stretchable, permeable, durable and washable fabric circuit boards, *Proceedings of the Royal Society A: Mathematical, Physical and Engineering Science* 470 (2014) <https://doi.org/10.1098/rspa.2014.0472>.
- [9] Q. Li, X. Tao, A stretchable knitted interconnect for three-dimensional curvilinear surfaces, *Text. Res. J.* 81 (2011) 1171–1182, <https://doi.org/10.1177/0040517511399965>.
- [10] Q. Li, Z.Y. Ran, X. Ding, X. Wang, Fabric circuit board connecting to flexible sensors or rigid components for wearable applications, *Sensors* 19 (2019).
- [11] A.N. Yang, Y.Z. Li, C.X. Yang, Y. Fu, N.X. Wang, L. Li, F. Yan, Fabric organic electrochemical transistors for biosensors, *Adv. Mater.* 30 (2018).
- [12] M.L. Scarpello, I. Kazani, C. Hertleer, H. Rogier, D. Vande Ginste, Stability and efficiency of screen-printed wearable and washable antennas, *IEEE Antennas and Wireless Propagation Letters* 11 (2012) 838–841, <https://doi.org/10.1109/Lawp.2012.2207941>.
- [13] R.B.V.B. Simorangkir, Y. Yang, K.P. Esselle, B.A. Zeb, A method to realize robust flexible electronically tunable antennas using polymer-embedded conductive fabric, *IEEE Trans. Antennas Propag.* 66 (2018) 50–58.
- [14] F. Wang, B. Zhu, L. Shu, X. Tao, Flexible pressure sensors for smart protective clothing against impact loading, *Smart Mater. Struct.* 23 (2014), 015001. <https://doi.org/10.1088/0964-1726/23/1/015001>.
- [15] C. Zysset, N. Nasserli, L. Buthe, N. Munzenrieder, T. Kinkeldei, L. Petti, S. Kleiser, G.A. Salvatore, M. Wolf, G. Troster, Textile integrated sensors and actuators for near-infrared spectroscopy, *Opt. Express* 21 (2013) 3213–3224, <https://doi.org/10.1364/Oe.21.003213>.
- [16] O. Atalay, W.R. Kennon, M.D. Husain, Textile-based weft knitted strain sensors: effect of fabric parameters on sensor properties, *Sensors* 13 (2013) 11114–11127, <https://doi.org/10.3390/S130811114>.
- [17] S. Takamatsu, T. Kobayashi, N. Shibayama, K. Miyake, T. Itoh, Fabric pressure sensor array fabricated with die-coating and weaving techniques, *Sensors and Actuators a-Physical* 184 (2012) 57–63, <https://doi.org/10.1016/j.sna.2012.06.031>.
- [18] L. Wang, K.J. Loh, Wearable carbon nanotube-based fabric sensors for monitoring human physiological performance, *Smart Mater. Struct.* 26 (2017).
- [19] M.C. Zhang, C.Y. Wang, H.M. Wang, M.Q. Jian, X.Y. Hao, Y.Y. Zhang, Carbonized cotton fabric for high-performance wearable strain sensors, *Adv. Funct. Mater.* 27 (2017).
- [20] W. Zeng, X.M. Tao, S. Chen, S.M. Shang, H.L.W. Chan, S.H. Choy, Highly durable all-fiber nanogenerator for mechanical energy harvesting, *Energy Environ. Sci.* 6 (2013) 2631–2638, <https://doi.org/10.1039/C3ee41063c>.
- [21] F. Peng, D. Liu, W. Zhao, G.Q. Zheng, Y.X. Ji, K. Dai, L.W. Mi, D.B. Zhang, C.T. Liu, C.Y. Shen, Facile fabrication of triboelectric nanogenerator based on low-cost thermoplastic polymeric fabrics for large-area energy harvesting and self-powered sensing, *Nano Energy* 65 (2019).
- [22] K. Jost, C.R. Perez, J.K. McDonough, V. Presser, M. Heon, G. Dion, Y. Gogotsi, Carbon coated textiles for flexible energy storage, *Energy Environ. Sci.* 4 (2011) 5060–5067, <https://doi.org/10.1039/C1ee02421c>.
- [23] S. Hong, Y. Gu, J.K. Seo, J. Wang, P. Liu, Y.S. Meng, S. Xu, R. Chen, Wearable thermoelectrics for personalized thermoregulation, *Sci. Adv.* 5 (2019) eaaw0536, <https://doi.org/10.1126/sciadv.aaw0536>.
- [24] J.W. Lee, R. Xu, S. Lee, K.-I. Jang, Y. Yang, A. Banks, K.J. Yu, J. Kim, S. Xu, S. Ma, S.W. Jang, P. Won, Y. Li, B.H. Kim, J.Y. Choe, S. Huh, Y.H. Kwon, Y. Huang, U. Paik, J.A. Rogers, Soft, thin skin-mounted power management systems and their use in wireless thermography, *Proc. Natl. Acad. Sci.* 113 (2016) 6131–6136, <https://doi.org/10.1073/pnas.1605720113>.
- [25] M. Cakici, K.R. Reddy, F. Alonso-Marroquin, Advanced electrochemical energy storage supercapacitors based on the flexible carbon fiber fabric-coated with uniform coral-like MnO<sub>2</sub> structured electrodes, *Chem. Eng. J.* 309 (2017) 151–158.
- [26] H. Tian, Y. Shu, X.-F. Wang, M.A. Mohammad, Z. Bie, Q.-Y. Xie, C. Li, W.-T. Mi, Y. Yang, T.-L. Ren, A graphene-based resistive pressure sensor with record-high sensitivity in a wide pressure range, *Sci. Rep.* 5 (2015) <https://doi.org/10.1038/srep08603>.
- [27] L. Wang, L.Y. Wang, Y. Zhang, J. Pan, S.Y. Li, X.M. Sun, B. Zhang, H.S. Peng, Weaving sensing fibers into electrochemical fabric for real-time health monitoring, *Adv. Funct. Mater.* 28 (2018).
- [28] C.P. Mao, H.H. Zhang, Z.S. Lu, Flexible and wearable electronic silk fabrics for human physiological monitoring, *Smart Mater. Struct.* 26 (2017).
- [29] S.C.B. Mannsfeld, B.C.K. Tee, R.M. Stoltenberg, C.V.H.H. Chen, S. Barman, B.V.O. Muir, A.N. Sokolov, C. Reese, Z.N. Bao, Highly sensitive flexible pressure sensors with microstructured rubber dielectric layers, *Nat. Mater.* 9 (2010) 859–864, <https://doi.org/10.1038/Nmat2834>.
- [30] C. Walsh, Human-in-the-loop development of soft wearable robots, *Nature Reviews Materials* 3 (2018) 78–80, <https://doi.org/10.1038/s41578-018-0011-1>.
- [31] S. Niu, N. Matsuhisa, L. Bekker, J. Li, S. Wang, J. Wang, Y. Jiang, X. Yan, Y. Yun, W. Burnett, A.S.Y. Poon, J.B.H. Tok, X. Chen, Z. Bao, A wireless body area sensor network based on stretchable passive tags, *Nature Electronics* 2 (2019) 361–368, <https://doi.org/10.1038/s41928-019-0286-2>.
- [32] X.W. Wang, Y. Gu, Z.P. Xiong, Z. Cui, T. Zhang, Silk-molded flexible, ultrasensitive, and highly stable electronic skin for monitoring human physiological signals, *Adv. Mater.* 26 (2014) 1336–1342, <https://doi.org/10.1002/adma.201304248>.
- [33] Y.M. Zhou, J.X. He, H.B. Wang, K. Qi, N. Nan, X.L. You, W.L. Shao, L.D. Wang, B. Ding, S.Z. Cui, Highly sensitive, self-powered and wearable electronic skin based on pressure-sensitive nanofiber woven fabric sensor, *Sci. Rep.* 7 (2017).
- [34] F.X. Yin, J.Z. Yang, H.F. Peng, W.J. Yuan, Flexible and highly sensitive artificial electronic skin based on graphene/polyamide interlocking fabric, *J. Mater. Chem. C* 6 (2018) 6840–6846.
- [35] W. Gong, C. Hou, J. Zhou, Y. Guo, W. Zhang, Y. Li, Q. Zhang, H. Wang, Continuous and scalable manufacture of amphibious energy yarns and textiles, *Nat. Commun.* 10 (2019) 868, <https://doi.org/10.1038/s41467-019-08846-2>.
- [36] L.M. Castano, A.B. Flatau, Smart fabric sensors and e-textile technologies: a review, *Smart Mater. Struct.* 23 (2014) <https://doi.org/10.1088/0964-1726/23/5/053001>.
- [37] X.T. Li, H.B. Hu, T. Hua, B.G. Xu, S.X. Jiang, Wearable strain sensing textile based on one-dimensional stretchable and weavable yarn sensors, *Nano Res.* 11 (2018) 5799–5811 (doi).
- [38] G.M. Cai, M.Y. Yang, Z.L. Xu, J.G. Liu, B. Tang, X.G. Wang, Flexible and wearable strain sensing fabrics, *Chem. Eng. J.* 325 (2017) 396–403 (doi).
- [39] Q. Li, L.N. Zhang, X.M. Tao, X. Ding, Review of flexible temperature sensing networks for wearable physiological monitoring, *Advanced Healthcare Materials* 6 (2017), 1601371. <https://doi.org/10.1002/adhm.201601371>.
- [40] J. Kim, A.S. Campbell, B.E.-F. de Ávila, J. Wang, Wearable biosensors for healthcare monitoring, *Nat. Biotechnol.* 37 (2019) 389–406, <https://doi.org/10.1038/s41587-019-0045-y>.
- [41] X. Wang, X. Tao, R.C.H. So, L. Shu, B. Yang, Y. Li, Monitoring elbow isometric contraction by novel wearable fabric sensing device, *Smart Materials & Structures* 25 (2016), 125022. <https://doi.org/10.1088/0964-1726/25/12/125022>.
- [42] X. Wang, X. Tao, R.C.H. So, A bio-mechanical model for elbow isokinetic and isotonic flexions, *Sci. Rep.* 7 (2017) 8919, <https://doi.org/10.1038/s41598-017-09071-x>.
- [43] D.R. Seshadri, R.T. Li, J.E. Voos, J.R. Rowbottom, C.M. Alfes, C.A. Zorman, C.K. Drummond, Wearable sensors for monitoring the internal and external workload of the athlete, *npj Digital Medicine* 2 (2019) 71, <https://doi.org/10.1038/s41746-019-0149-2>.
- [44] Y. Li, F. Guo, Y. Hao, S.K. Gupta, J. Hu, Y. Wang, N. Wang, Y. Zhao, M. Guo, Helical nanofiber yarn enabling highly stretchable engineered microtissue, *Proc. Natl. Acad. Sci.* 116 (2019) 9245–9250, <https://doi.org/10.1073/pnas.1821617116>.
- [45] L. Shu, T. Hua, Y.Y. Wang, Q.A. Li, D.D. Feng, X.M. Tao, In-shoe plantar pressure measurement and analysis system based on fabric pressure sensing array, *IEEE Trans. Inf. Technol. Biomed.* 14 (2010) 767–775, <https://doi.org/10.1109/TITB.2009.2038904>.

- [46] L. Viry, A. Levi, M. Totaro, A. Mondini, V. Mattoli, B. Mazzolai, L. Beccai, Flexible three-axial force sensor for soft and highly sensitive artificial touch, *Adv. Mater.* 26 (2014) 2659–2664, <https://doi.org/10.1002/adma.201305064>.
- [47] Z. Wang, C. Xiang, X. Yao, P. Le Floch, J. Mendez, Z. Suo, Stretchable materials of high toughness and low hysteresis, *Proc. Natl. Acad. Sci.* 116 (2019) 5967–5972, <https://doi.org/10.1073/pnas.1821420116>.
- [48] S. Lee, M. Pharr, Sideways and stable crack propagation in a silicone elastomer, *Proc. Natl. Acad. Sci.* 116 (2019) 201820424, <https://doi.org/10.1073/pnas.1820424116>.
- [49] M.S. Al-Haik, H. Garmestani, A. Savran, Explicit and implicit viscoplastic models for polymeric composite, *Int. J. Plast.* 20 (2004) 1875–1907, <https://doi.org/10.1016/j.ijplas.2003.11.017>.
- [50] O. Graudejus, P. Gorn, S. Wagner, Controlling the morphology of gold films on poly (dimethylsiloxane), *ACS Appl. Mater. Interfaces* 2 (2010) 1927–1933, <https://doi.org/10.1021/Am1002537>.
- [51] H. Park, J.S. Lee, S. Kwon, S. Yoon, D. Kim, Effect of surface morphology on screen printed solar cells, *Curr. Appl. Phys.* 10 (2010) 113–118, <https://doi.org/10.1016/j.cap.2009.05.005>.
- [52] T. Yamada, M. Matsuo, The study of effect of a polyurethane filament on mechanical properties of plain stitch fabrics, *Text. Res. J.* 79 (2009) 310–317, <https://doi.org/10.1177/0040517508090501>.
- [53] G. Dusserre, Modelling the hysteretic wale-wise stretching behaviour of technical plain knits, *European Journal of Mechanics - A/Solids* 51 (2015) 160–171, <https://doi.org/10.1016/j.euromechsol.2014.12.009>.
- [54] M. Matsuo, T. Yamada, Hysteresis of tensile load – strain route of knitted fabrics under extension and recovery processes estimated by strain history, *Text. Res. J.* 79 (2009) 275–284, <https://doi.org/10.1177/0040517507090504>.
- [55] L. Guo, L. Berglin, H. Mattila, Improvement of electro-mechanical properties of strain sensors made of elastic-conductive hybrid yarns, *Text. Res. J.* 82 (2012) 1937–1947, <https://doi.org/10.1177/0040517512452931>.
- [56] T. Matsuda, S. Kanamaru, N. Yamamoto, Y. Fukuda, A homogenization theory for elastic-viscoplastic materials with misaligned internal structures, *Int. J. Plast.* 27 (2011) 2056–2067, <https://doi.org/10.1016/j.ijplas.2011.05.016>.
- [57] R. Liu, T.T. Lao, S.X. Wang, Impact of weft laid-in structural knitting design on fabric tension behavior and interfacial pressure performance of circular knits, *Journal of Engineered Fibers and Fabrics* 8 (2013), 155892501300800404. <https://doi.org/10.1177/155892501300800404>.
- [58] B. Niu, T. Hua, H. Hu, B. Xu, X. Tian, K. Chan, S. Chen, A highly durable textile-based sensor as a human-worn material interface for long-term multiple mechanical deformation sensing, *J. Mater. Chem. C* 7 (2019) 14651–14663.
- [59] T. Yamada, Y. Hayamizu, Y. Yamamoto, Y. Yomogida, A. Izadi-Najafabadi, D.N. Futaba, K. Hata, A stretchable carbon nanotube strain sensor for human-motion detection, *Nat. Nanotechnol.* 6 (2011) 296–301, <https://doi.org/10.1038/Nnano.2011.36>.
- [60] Y. Xiong, X. Tao, Compression garments for medical therapy and sports, *Polymers* 10 (2018) 663, <https://doi.org/10.3390/polym10060663>.
- [61] W. Li, S. Yang, A. Shamim, Screen printing of silver nanowires: balancing conductivity with transparency while maintaining flexibility and stretchability, *npj Flexible Electronics* 3 (2019) 13, <https://doi.org/10.1038/s41528-019-0057-1>.
- [62] F. Carpi, D. De Rossi, Electroactive polymer-based devices for e-textiles in biomedicine (vol 9, pg 295, 2005), *IEEE Trans. Inf. Technol. Biomed.* 9 (2005) 574, <https://doi.org/10.1109/Titb.2005.858429>.
- [63] A.M. Grancaric, I. Jerkovic, V. Koncar, C. Cochrane, F.M. Kelly, D. Soulat, X. Legrand, Conductive polymers for smart textile applications, *J. Ind. Text.* 48 (2018) 612–642.
- [64] G. Paul, R. Torah, K. Yang, S. Beeby, J. Tudor, An investigation into the durability of screen-printed conductive tracks on textiles, *Meas. Sci. Technol.* 25 (25006) (2014) 1–11, <https://doi.org/10.1088/0957-0233/25/2/025006>.
- [65] C.T. Lan, C.L. Li, J.Y. Hu, S.G. Yang, Y.P. Qiu, Y. Ma, High-loading carbon nanotube/polymer nanocomposite fabric coatings obtained by capillarity-assisted “excess assembly” for electromagnetic interference shielding, *Adv. Mater. Interfaces* 5 (2018).
- [66] M. Chen, P.W. Gao, F. Geng, L.F. Zhang, H.W. Liu, Mechanical and smart properties of carbon fiber and graphite conductive concrete for internal damage monitoring of structure, *Constr. Build. Mater.* 142 (2017) 320–327.
- [67] Y.J. Zheng, Y.L. Li, K. Dai, Y. Wang, G.Q. Zheng, C.T. Liu, C.Y. Shen, A highly stretchable and stable strain sensor based on hybrid carbon nanofillers/polydimethylsiloxane conductive composites for large human motions monitoring, *Compos. Sci. Technol.* 156 (2018) 276–286.
- [68] J.G. Simmons, Electric tunnel effect between dissimilar electrodes separated by a thin insulating film, *J. Appl. Phys.* 34 (1963) 2581–2590.